Published in final edited form as:
Biochemistry. 2012 September 4; 51(35): 6990–6999. doi:10.1021/bi3008824.

Human Brown Fat Inducible Thioesterase *Variant 2* (BFIT2) Cellular Localization and Catalytic Function#

Danqi Chen[‡], **John Latham**[‡], **Hong Zhao**[‡], **Marco Bisoffi**[§], **Jeremiah Farelli**[+], and **Debra Dunaway-Mariano**[‡,*]

[‡]Department of Chemistry and Chemical Biology University of New Mexico, Albuquerque, New Mexico

[§]Department of Biochemistry and Molecular Biology, University of New Mexico Health Sciences Center, Albuquerque, New Mexico

[+]Department of Chemistry, Boston University, Boston, Massachusetts, USA 02215.

Abstract

The mammalian brown fat inducible thioesterase variant 2 (BFIT2), also known as ACOT11, is a multi-modular protein containing two consecutive hotdog-fold domains and a C-terminal steroidogenic acute regulatory protein related lipid transfer (START) domain (StarD14). In this study, we demonstrate that the N-terminal region of human BFIT2 (hBFIT2) constitutes a mitochondrial location signal sequence, which undergoes mitochondria-dependent posttranslational cleavage. The mature hBFIT2 is shown to be located in the mitochondrial matrix whereas the paralog “cytoplasmic acetyl-CoA hydrolase” (CACH, also known as ACOT12) was found in the cytoplam. *In-vitro* activity analysis of full-length hBFIT2 isolated from stably transfected HEK293 cells demonstrates selective thioesterase activity directed towards long chain fatty acyl-CoA thioesters, thus distinguishing BFIT2 catalytic function from that of CACH. The results from a protein-lipid overlay test indicate that the hBFIT2 StarD14 domain binds phosphatidylinositol 4-phosphate.

Keywords

thioesterase; mitochondria; START domain; hotdog-fold; thioester hydrolysis; lipid metabolism; ACOT11; ACOT12; BFIT; CACH; StarD14; StarD15; fatty acid

Body heat production triggered by low temperature or a high fat diet is known as adaptive thermogenesis (1-4). In brown fat adipose tissue (BAT),[1] thermogenesis is associated with the decoupling of energy metabolism and ATP synthesis *via* the action of the mitochondrial transmembrane protein UCP1 (5-9). UCP1 allows the protons that have been pumped into

[#]Supported by NIH Grant GM28688

[*]Corresponding Author: Debra Dunaway-Mariano MSC03 2060; 1 University of New Mexico Albuquerque, New Mexico 87131. Tel.: 505.277.3383; Fax: 505.277.2609; dd39@unm.edu.

SUPPORTING INFORMATION

Detailed experimental protocol and tables and figures reporting experimental results or protein graphics are available free of charge via the Internet at http://pubs.acs.org

the mitochondrial intermembrane space by the electron transport system, transport to the mitochondrial matrix thus side-stepping the membrane ATP synthase. The energy potential intended to drive ATP synthesis is instead released as heat. Because fatty acid oxidation feeds the electron transport system the observation that thermogenesis is accompanied by increased expression of genes encoding proteins for *de novo* fatty acid synthesis, fatty acid β-oxidation and lipogenesis is not surprising (10-11). Among these up-regulated genes is the gene, which encodes the brown fat inducible thioesterase ("BFIT").

The human BFIT exists in two splice forms hBFIT1 and hBFIT2, whereas in mice a single splice form that corresponds to the hBFIT2 exists. In mice and in human infants brown adipose tissue (BAT) mediates nonshivering thermogenesis. In a very recent study, it was observed that mBFIT gene-knockout mice are resistant to diet-induced obesity despite greater food consumption (12). The mice displayed an array of physiological and metabolic changes, which included, but were not limited to, increased O_2 consumption, heat production and β-fatty acid oxidation, improved glucose homeostasis and attenuated endoplasmic reticulum stress response. These changes were posited to be BAT-mediated responses. In human adults, where the amount of BAT is comparatively low (13-15), it is thought that BFIT may perform a more generalized function as a regulator of energy homeostasis (12). Notably, BFIT is ubiquitously expressed in human tissues. The hBFIT1 variant is predominant in skeletal muscle, liver, testis, stomach, spleen, lung, and brain, whereas the hBFIT2 variant is predominant in kidney, uterus, hibernoma, and white adipose tissue (13). Both variants are expressed equally in heart tissue (13).

Based on its amino acid sequence, BFIT is predicted to be a large modular protein comprised of two consecutive hotdog-fold units followed by a steroidogenic acute regulatory protein related lipid transfer (START) domain (16-17) (Figure 1A). The hotdog-fold defines the tertiary structure of a large family of functionally diverse enzymes (18-28). Among the chemical function subfamilies, is the thioesterase subfamily (29-31). Although as named, BFIT is presumed to be a thioesterase, there are no published activity data to support this subfamily assignment (32).[2] The biological unit of the typical hotdog-fold enzyme is a dimer of a small α,β-folding subunit that is best described as a long α-helix ("sausage") wrapped by a twisted, 5-6 strand β-sheet ("bun"). In a small, but significant fraction of the hotdog-fold proteins, the two subunits of the dimer are connected to form the "double" hotdog-fold, as is predicted for BFIT. To illustrate this fold, a representative structure, that of the engineered double hotdog-fold domain of the sequence homolog cytoplasmic acetyl-CoA hydrolase (CACH, also known as ACOT12), is shown in Figure

[1]Abbreviations used include: human or mouse brown fat inducible thioesterase (hBFIT or mBFIT); brown adipose tissue (BAT); coenzyme A (CoA); steroidogenic acute regulatory protein related lipid transfer (START); cytoplasmic acetyl-CoA hydrolase (CACH), aminotris(hydroxymethyl)methane (Tris); phosphate buffered saline (PBS); 4-(2-hydroxyethyl)-1-piperazineethanesulfonic acid (HEPES); polyethylene glycol (PEG); electrospray ionization mass spectrometry (ES-MS); mitochondrial localization sequence (MLS); green fluorescent protein (GFP); high performance liquid chromatography (HPLC); dithionitrobenzene (DTNB)

[2]The reference cited for the demonstration of BFIT thioesterase activity is: BFIT, a unique acyl-CoA thioesterase induced in thermogenic brown adiopose tissue: cloning, organization of the human gene and assessment of a potential link to obesity. Sean H. Adams *et al.*, *Biochemical Journal 360*, 135-142 (2001). In this paper the following statement appears in the discussion section: "The thioesterase domain structure of BFIT, coupled to its protein sequence homology with a broad range of acyl-CoA thioesters (see Results), suggested that this enzyme catalyses hydrolytic thioester cleavage, thus yielding non-esterified fatty acids (NEFAs) and CoA. Consistent with this, initial assays using partially purified *Escherichia coli*-generated recombinant hBFIT proteins displayed acyl-CoA thioesterase activity towards a medium (C_{12}-CoA) and a long-chain (C_{16}-CoA) fatty acyl-CoA substrate (S.H Adams, R. Vandlen and D. Yansura, unpublished work)." To our knowledge this "unpublished work" has not been published.

1B. The enzyme functions that have been identified for double hotdog-fold proteins include thioesterase (33), dehydratase (34), decarboxylase (35), hydratase (36) and β-ketoacyl transfer (37). In human, the thioesterase and dehydratase activities are required for lipid metabolism.

Members of the START family are standalone proteins or domains within a larger modular protein, as exemplified by BFIT (17). The physiological ligands of only a fraction of the members of this family (viz). StarD1 (38-39), StarD2 (PC-TP) (40), StarD3 (MLN64) (41-42), StarD7 (43-44) and StarD11 (CERT) (45)) have been identified. Known START ligands include cholesterol (StarD1, 3, 4, 5 and 6), ceramides (Stard11) phosphatidyl ethanolamine (StarD10) and/or phosphatidyl choline (StarD2 and 7). The X-ray structure of the hBFIT2 START domain (StarD14) is shown in Figure 1C (46). It, like other START protein X-ray structures, possesses the characteristic curved β-sheet that is gripped by four α-helices (highlighted in Figure 1C) (46). The α4-helix (colored green in Figure 1C) acts as a lid over the ligand binding sites of the START domains. To allow the ligand access to the binding site, the α4-helix must presumably move out of the way. The identity of the StarD14 physiological ligand has not been demonstrated, although based on the X-ray crystal structure, which was modeled with a solvent polyethylene glycol (PEG) molecule at the putative binding site, it has been suggested that it might be a fatty acid (46).

As part of our program to define structure, function and mechanism in human hotdog-fold thioesterases (19-20), we have targeted hBFIT2 for study. Our first objective was to determine its cellular compartmentalization and biochemical activity. Herein, we report our findings that show that recombinant hBFIT2 produced in human HEK293 cells is translocated to the mitochondrial matrix and that the purified protein targets long chain fatty acyl-CoA thioesters for catalyzed hydrolysis. In addition, we report the preliminary results from a protein-lipid overlay assay, which suggest that the StarD14 domain binds phosphatidylinositol 4-phosphate.

Materials and Methods

Reagents

HEK293T/17 cell line, Dulbecco's modified Eagle's medium, fetal bovine serum and the Trypsin-EDTA reagent were purchased from the American Type Culture Collection (ATCC) (Manassas, VA). Transfection and stable cell line selection reagents OptiMEM, Zeocin, Lipofectamine 2000 and phosphate buffered saline (PBS), were purchased from Invitrogen (Carlsbad, CA). The mitochondria isolation kit for cultured cells and the direct immunoprecipitation kit were purchased from Pierce (Rockford, IL). Mammalian expression vectors, including pcDNA4 HisMAX TOPO, pcDNA3.1 CT-GFP TOPO and pcDNA3.1 NT-GFP TOPO, were purchased from Invitrogen. Anti-hBFIT2 antibody was purchased from Abcam (Cambridge, MA), anti-mouse mHSP70 and anti-mouse AIF antibodies were purchased from Thermo Scientific (Waltham, MA). Other antibodies, including mouse anti-Xpress, anti-HisG, anti-α tubulin, and anti-mouse HRP, were purchased from Invitrogen. The nuclear extraction kit was purchased from Active Motif (Carlsbad, CA). Cellular compartment dyes mitotracker Red CMXRos, WGA/Alexa Fluor 594 conjugate and

Hoechst 33342 were purchased from Invitrogen. All other reagents were purchased from Sigma-Aldrich unless otherwise indicated.

Expression Vectors and Transfection of HEK293T/17 Cells

A PCR-based strategy was used to amplify the cDNA region encoding full-length hBFIT2 (Openbiosystem), ΔN-terminal MLS hBFIT2 (minus amino acid residues 1-34 amino acids) or the hBFIT2 N-terminal MLS (amino acids 1-42). Following the addition of the 3'-end adenine hangover using platinum *Taq* polymerase (Invitrogen), the respective PCR products were cloned into TOPO expression vectors. The resulting plasmids, including hBFIT2/pcDNA4 HisMAX, hBFIT2 (ΔN 34)/pcDNA4 HisMAX, hBFIT2/pcDNA3.1 NT-GFP, hBFIT2/pcDNA3.1 CT-GFP and *hBFIT2 (N 1-42)/pcDNA3.1 CT-GFP*, were used to transfect HEK293T/17 cells. For transient transfection, HEK293T/17 cell lines were plated in 24-well or 6-well plates and transfected the following day at 80% confluency according to the manufacturer's instruction. For *hBFIT2/pcDNA4 HisMAX* stably transfected cell lines, selections were carried out in culture medium containing 500 μg/mL Zeocin.

Immunoblot Analysis

Extracts from the lysates of transfected or untransfected HEK293T/17 cells were prepared by using a nuclear extraction kit or an immunoprecipitation lysis/wash buffer (Pierce) according to the manufacturer's instructions. The total protein concentration was measured by using the Bradford assay. The proteins were separated by SDS-PAGE using 12% polyacrylamide gels and then transferred to nitrocellulose membranes. Next, the membranes were treated with primary antibody for ~15 h at 4 °C. After extensive washing, the membrane was treated with anti-mouse HRP. Finally, imaging was carried out using enhanced chemical luminescent reagents (Perkin Elmer).

Immunoprecipitation of hBFIT2

Anti-Xpress or anti-HisG antibody covalently immobilized agarose beads were prepared following the manufacturer's instruction. In brief, 10-50 μg of primary antibody was incubated with 20-100 μL of an agarose bead slurry in the presence of $NaCNBH_3$ at room temperature for 2-3 h. Uncoupled antibody was removed by extensive washing with lysis/wash buffer (25 mM Tris pH7.4, 0.15M NaCl, 0.001M EDTA, 1% NP-40 and 5% glycerol) and uncoupled reaction sites on the agarose beads were quenched by quench buffer (1 M Tris) and $NaCNBH_3$. The lysate of *hBFIT2/pcDNA4 HisMAX* stably transfected HEK cells was incubated with antibody-immobilized agarose beads at 4 °C for ~15 h. Unbound proteins were removed by washing the beads with lysis/washing buffer. Finally, the hBFIT2 was eluted from the beads with 10 mM Tris/100 mM glycine (pH 7.4).

Confocal Imaging of GFP Fusion Protein

HEK293T/17 cells were cultured on a coverslip and transfected with GFP fusion expression plasmids. After 12-24 h post-transfection, the cells were fixed using 4% polyformaldehyde in PBS buffer at 37 °C for 15 min. Subsequently, the fixed cells were incubated with 1 μM Hoechst 33342 and either 50 μM Mitotracker Red CMXRox or 5 μg/mL WGA/Alexa Fluor 594 conjugate at room temperature for 20 min. Finally, the coverslip was rinsed with PBS,

mounted onto slides, and subjected to confocal microscope analysis (Cancer Center Fluorescence Microscopy Facility, University of New Mexico School of Medicine).

Mitochondrial Fraction Isolation from HEK293T/17 Cells

Mitochondria isolation was performed with a Thermoscientific (IL, USA) mitochondrial isolation kit by following the manufacturer's instructions. In brief, ~2 × 10^7 untransfected or *hBFIT2/pcDNA4 HisMAX* stably transfected HEK293T/17 cells were harvested by centrifugation and then resuspended in mitochondria isolation reagent A. Cells were lysed by using a Dounce tissue grinder. Mitochondria isolation reagent C was added to the cell lysate. Cytosolic and mitochondrial fractions were separated by centrifugation. The pelleted mitochondria were washed once with reagent C and then resuspended in a suitable buffer for downstream processing.

In vitro Processing and Importing of hBFIT2 by Freshly Isolated Mitochondria from Untransfected HEK293T/17 Cells

Precursor (full-length) hBFIT2 was isolated by immunoprecipitation. A posttranslational processing assay was performed in the following manner. Six milligrams of freshly isolated mitochondria were resuspended in 150 μL of 2X mannitol buffer (450 mM mannitol, 50 mM sucrose, 20 mM Tris, 0.2 mM EDTA, 100 mM ATP, 10 mM $MgCl_2$, 160 mM KCl, 0.2 mM pyruvate and 360 mM malate). After the addition of 0.6 μg of hBFIT2 in a volume of 150 μL and incubation at room temperature for 10 min, the temperature was increased to 37 °C. Eighty microliter aliquots were removed after 5, 30, and 60 min, heated in boiling water bath for 10 min and then chromatographed on a SDS-PAGE gel. The protein was transferred from the gel to a nitrocellulose membrane, which in turn was subjected to Western blot analysis.

For the *in-vitro* mitochondrial import assay, hBFIT2 was incubated with mitochondria as described above. Aliquots of reaction mixture were removed after 5, 30 and 60 min. Supernatant and pellet (mitochondria) were separated and then subjected to Western blot analysis.

In-silico Analysis of the N-Terminal Region of hBFIT2

An EMBOSS pepwheel helical wheel plot (http://150.185.138.86/cgi-bin/emboss/pepwheel) was utilized to investigate the amphipathy of the N-terminal region (amino acid 1-42 residues) of hBFIT2. The sequence alignment was generated by using ClustalW2 (http://www.ebi.ac.uk/Tools/msa/clustalw2/). The tertiary structure prediction of the N-terminal region of hBFIT2 was carried out with the Protein homology/analogy recognition engine PHYRE2 (http://www.sbg.bio.ic.ac.uk/phyre2/html/page.cgi?id=index).

MALDI-TOF Mass Spectrometry Analysis of BFIT2

A sample of hBFIT2 for mass spectral analysis was obtained by immunoprecipitation from *hBFIT2/pcDNA4 HisMAX* stably transfected HEK293T/17 cells by using anti-Xpress antibody. Following SDS-PAGE chromatography, the protein sample was subjected to trypsin digestion and subsequent MALDI-TOF mass spectrometry analysis. Signature peptides were searched against those in the protein data bank by using MASCOT server for

protein identity confirmation (Protein Analysis Facilities, Skirball institute at the New York University School of Medicine)

Digitonin Treatment of a Mitochondrial Fraction Freshly Obtained From BFIT2 Stably Transfected HEK293T/17 Cells

Mitochondrial fractions of hBFIT2 in stably transfected HEK293T/17 cells were isolated using the method described previously (*vide supra*). The fractions, resuspended in mannitol buffer at a *w/v* of 1 mg/mL, were treated with digitonin in the concentration range of 0 to 0.6 mg/mL at 4 °C for 45 min. The pellet (mitochondria) fraction obtained by centrifugation at 20,000 × g, was subjected to Western blot analysis using anti-mHSP70, anti-AIF and anti-Xpress (for hBFIT2 detection) antibodies.

Scale-up Culture of hBFIT2/pcDNA 4 HisMAX and or hCACH/pcDNA4 HisMAX Stably Transfected HEK293T/17 Cell Line and Purification of hBFIT2 and hCACH

The plasmids *hBFIT2/pcDNA4 HisMAX* and *hCACH/pcDNA4 HisMAX* were separately used to transiently transfect HEK293T/17 cells. Selection of stably transfected HEK293T/17 cell colonies was performed using the antibiotic Zeocin at a concentration of 300 μg/mL. A cell stock was prepared from a single stably transfected HEK cell by culturing in a single well of a 6-well plate in the presence of 100 μg/mL of Zeocin until the confluency reached 90%. The cells were then detached by trypsin treatment and passed into four 150 mm plates. Two more passages with a ratio of 1:4 were performed when the cell cultures achieved 90% confluency. The HEK cells from sixty-four 150 mm plates were collected by scraping, and then stored at -80%. After treating the cells with two freeze-and-thaw cycles, the mixture was centrifuged and the resulting supernatant was collected for purification. Immunoprecipitation was carried out as described above. The recombinant protein was eluted from the antibody-coated beads with elution buffer (1M Tris, pH 7.5). The hBFIT2 was dialyzed overnight at 4 °C against storage buffer (50 mM Tris/50 mM NaCl, pH 7.5). When Ni-NTA affinity purification was used to isolate the recombinant protein, the supernatant was gradually loaded to 3 mL Ni-NTA column. After extensively washing of the column with 50 mM imidazole, the recombinant protein was eluted with 250 mM imidazole. The eluted recombinant protein was dialyzed at overnight 4 °C against storage buffer. The recombinant protein concentration was determined by measuring the nanodrop absorbance at 280 nm (hBFIT2: 70820 $M^{-1}cm^{-1}$ and hCACH: 71390 $M^{-1}cm^{-1}$). The recombinant protein homogeneity was confirmed by ES-MS and by SDS-PAGE chromatography followed by transfer to a nitrocellulose membrane, which in turn was subjected Western blot analysis and Coomassie Blue staining.

Cloning and Expression of the ybdB Thioesterase Gene and Purification of the Protein Product

The gene encoding *E. coli* ybdB (47) was cloned into the pcDNA4 HisMAX TOPO vector and the resulting plasmid *ybdb/pcDNA4 HisMAX* was used as template in the PCR amplification of the ybdB gene fused at the first codon to the codons encoding the Xpress and HisG tags (Herein referred to as *tag-ybdb*). After gene cleaning, digestion treatment and ligation, the *tag-ybdb/pET23a* plasmid was prepared and utilized in the transformation of

competent *E. coli* BL21(DE3) cells. The recombinant protein was expressed in high yield and purified to homogeneity by Ni-NTA affinity column chromatography.

Protein-Lipid Overlay Assay

Each Membrane Lipid Strip (Echelon Bioscience Inc.) was treated with PBS containing 0.1% Tween 20 (PBS-T) and 3% BSA for at least 1 h prior to incubating with 0.5 μg/mL hBFIT2, 0.1 μg/mL hCACH or 6 μg/mL ybdB in PBS-T with 3% BSA for 1.5 h. After washing the strip 3 times with PBS-T buffer, it was incubated at room temperature with 1:2000 primary antibody (anti-HisG) for 1 h and then with 1:2000 secondary antibody (anti-mouse IgG) for 1h. Visualization of lipid-protein complex was performed by using the Western Lightning Chemiluminescent Reagent Plus kit (PerkinElmer) in conjunction with X-ray autoradiography.

HPLC Analysis of Thioesterase Activities of BFIT2 towards Acyl-CoA Thioesters

Commercial palmitoyl-, myristoyl, lauroyl- and butyryl-CoA thioesters were tested as substrates for hBFIT2. The 200 μL reaction solution initially containing 50 mM HEPES (pH 7.5), 50 μM NaCl, 50 μM acyl-CoA thioester and 0.34 μM BFIT2 was incubated at 37 °C. Aliquots (50 μL) were removed at 30 min and at 60 min and passed through an Amicon YM-10 (Millipore) filter. The control sample (no hBFIT2) was incubated at 37 °C for 2 h. The filtrates were analyzed by reversed-phase HPLC (UV detection wavelength at 260 nm) using a C18 reversed-phase column (5 μm, 4.6 mm × 25 cm) and a linear gradient of 0 to 65% acetonitrile in 20 mM $(NH_4)_2HPO_4$ buffer (pH 6.7).

Results and Discussion

BFIT2 Cellular Localization

The *hBFIT2/pcDNA4 HisMAX*-transfected HEK293T/17 cells synthesized recombinant hBFIT2 possessing the N-terminal epitopes HisG (H_6G) and Xpress (DLYDDDDK). These “tags” were added to facilitate protein purification and immunoblot detection. Immunoblot analysis of the transfected cell lysates carried out with anti-Xpress or anti-HisG antibodies revealed a single protein with an approximate mass of 71 kDa (hereafter referred to as precursor hBFIT2) (Figure 2), which matches the predicted value of recombinant full-length hBFIT2. The use of the anti-hBFIT2 antibody on the other hand, uncovered an additional protein with an approximate mass of 66 kDa (hereafter referred to as mature hBFIT2) (Figure 2), which we suspected to be a truncated form of the precursor hBFIT2. The identity and sequence integrity of the recombinant precursor hBFIT2 was examined by first isolating the full-length protein by immunoprecipitation using anti-Xpress antibody immobilized agarose beads (immunoblot is shown in Figure SI1). Proteolytic digestion of the protein sample yielded 25 fingerprint peptides, covering 33% of the total hBFIT2 sequence. These include the intact N-terminal region following the Xpress epitope, parts of internal sequence and the C-terminal region (Table SI1).

Having verified the identity of the precursor hBFIT2, our attention turned to characterization of the mature hBFIT2. Because the mature form escaped detection by the antibodies directed against the N-terminal epitopes, it was evident that the N-terminal region of the precursor

hBFIT2 had been cleaved. Indeed, the N-terminal region was predicted with 0.97 probability by the server MitoProt II (http://ihg.gsf.de/ihg/mitoprot.html) to contain a mitochondrial localization sequence (MLS). The putative cleavage site is located at residue 25. Tertiary structure prediction of the N-terminal region (residues 1-42) indicated a turn-coil-helix-turn-coil conformation (Figure 3A). The central α-helix, together with its adjacent coil (residues 9-24), is amphipathic: one face is exclusively hydrophilic/positively charged and the opposite face is mainly nonpolar/hydrophobic (Fig. 3B). The EMBOSS pepwheel diagram of the central α-helix also shows the concentration of nonpolar residues on one face and the polar residues on the opposite face (Fig. 3C). An alignment of N-terminal sequences of hBFIT2 from various mammalian species indicates a high degree of conservation across species (Fig. 3D). Specifically, residues with positive charge, including Arg10, Arg11, Arg20, Arg23 and Lys24 are stringently conserved. Furthermore, this region is also enriched with conserved hydroxyl group-carrying residues, including Ser15, Ser18, Thr21, Ser22 and Ser25. The preponderance of positive charged and hydroxyl group-carrying residues are characteristic of a MLS. Notably, the putative MLS is not present in the human sequence homolog CACH (“cytoplasmic acetyl-CoA hydrolase” also known as ACOT12) (48) (see Figure SI2 for the pairwise sequence alignment).

Proteins carrying a MLS are imported to mitochondria via mitochondrial translocases and subsequently processed by the matrix processing peptidase (49-51). To demonstrate that hBFIT2 possesses a functional MLS at the N-terminal region, the encoding gene was engineered for expression of the HisG-tagged N-terminal truncate ΔN-34 hBFIT2 (residues 1-34). Immunoblot analysis of the transfected cell lysate using either anti-Xpress or anti-hBFIT2 antibody detected only one protein with MW ~68 kDa, close to the predicted value of ΔN-34 hBFIT2, indicating the abolishment of the posttranslational process (Fig. SI2). Next, the *hBFIT2 N(1-42)/pcDNA 3.1 CT-GFP* construct was prepared for expression of the BFIT2 N-terminal region (residues 1-42) in fusion with the green fluorescent protein (GFP). Transfected cells were fixed and stained for analysis with a confocal microscope. Whereas the GFP alone displayed distributive localization in the cell (Figure 4), the hBFIT2 N(1-42)-GFP exhibited patterned punctuate localization that coincides with the locations of the Mitotracker Red CMXRos stained mitochondria (Figure 4). Attempts to image the hBFIT2-GFP fusion protein failed owing to the formation of inclusion bodies. The CACH-GFP construct was, on the other hand, well behaved, and consistent with the prediction of the absence of a MLS, the CACH fusion protein displayed distributive localization in the cell (Figure 4).

Having verified the hBFIT2 MLS, our next step was to demonstrate that hBFIT2 is translocated from the cytoplasm to the mitochondria. Firstly, affinity purified precursor hBFIT2 was treated at 37 °C with mitochondria that were freshly isolated from HEK 293T/17 cells and freed of the cytoplasmic fraction (Fig. 5A). Immunoblot analysis of an aliquot of the incubation mixture revealed the formation of mature hBFIT2 (Fig. 5B). Secondly, the remainder of the incubation mixture was separated into the mitochondrial fraction and supernatant fraction. Immunoblot analysis of the two fractions revealed the presence of hBFIT2 in the mitochondrial fraction only (Fig. 5C). Taken together, these

results show that precursor hBFIT2 is translocated to the mitochondria where the MLS is removed by the action of the matrix processing peptidase.

To determine if hBFIT2 localizes within the mitochondrial matrix or remains in the intermembrane space, mitochondria isolated from hBFIT2 stably transfected HEK293T/17 cells were treated with digitonin. A low concentration (0.05-0.20 mg/mL) of digitonin permeates the outer membrane of mitochondria and releases protein localized in the intermembrane space, whereas a higher concentration (0.4-0.60 mg/mL) of digitonin is needed to release matrix proteins. AIF and mHSP70 were used as protein markers for release of intermembrane proteins and matrix proteins, respectively. Figure 6 shows that the majority of the AIF was released at 0.20 mg/mL of digitonin whereas the majority of the hBFIT2 and mHSP70 remained at 0.6 mg/mL digitonin. We concluded that mature hBFIT2 is likely to reside in the mitochondrial matrix protein barring posttranslational modification that might direct it to the nucleus or that might silence the MLS, thus confining the precursor hBFIT2 to the cytoplasm. Notably, when queried with the BFIT2 amino acid sequence, the search engine SUMOplot (http://www.abgent.com/tools/sumoplot) did not detect a sumoylation site whereas the search engine NetPhos 2.0 (http://www.cbs.dtu.dk/services/NetPhos/) predicted the MLS Ser22 and Ser25 as kinase phosphorylation sites with the high score of 0.997. If the MLS Ser residues are in fact subject to protein kinase phosphorylation/phosphatase dephosphorylation, it follows that the location of hBFIT2 (cytoplasm *vs* mitochondrial matrix) is subject to regulation via phosphorylation (52).

Enzymatic Activity

Having identified the likely cellular location of native hBFIT2 (*viz.* precursor form: cytoplasm and mature form: mitochondrial matrix)[3] the next step was to characterize its enzymatic activity. The closest homolog to hBFIT2 is CACH (ACOT12). The rat ACOT12 ortholog was previously shown to specifically catalyze the hydrolysis of acetyl-CoA (48, 53). We used the X-ray structure of the double hotdog-fold domain of the human ACOT12 (PDB ID: 3B7K) to generate a model of the corresponding hBFIT2 domain (60% sequence identity) so to compare active site residues. The model shows that hBFIT2 conserves the ACOT12 catalytic motif residues (Figure 7). The BFIT2 residues are the α—helix N terminus residues Gly67 (active site 1) and Gly239 (active site 2) and the central α—helix carboxylate residues Asp74 (active site 1) and Glu247 (active site 2). The backbone amide NH of the α—helix N terminus residue is known to function in hotdog-fold thioesterases to form a hydrogen bond with the substrate thioester carbonyl oxygen atom, thereby activating the carbonyl carbon atom for nucleophilic attack (26). The α—helix carboxylate residue is on the other hand, known to function in nucleophilic (29) or base catalysis (20).

Building on the hypothesis that hBFIT2 is a thioesterase we focused the catalytic activity tests on the hydrolysis of fatty acyl-CoA thioesters, the substrates for mitochondrial fatty acid β-oxidation. In order to execute the activity assays we needed the purified hBFIT2. However, all attempts at using *E. coli* or yeast as a platform for hBFIT2 production failed,

[3]The conversion of the recombinant hBFIT2 from the precursor form to the mature form in the mitochondria did not go to completion, which we attribute to the N-terminal tags and/or the artificial environment associated with the *in-vitro* assay. The native hBFIT2, is expected to be completely processed by the mitochondria in the cell.

and therefore we opted to grow numerous batches of the stably transfected HEK293T/17 cells to provide a limited supply of the pure recombinant protein for testing against a prioritized panel of fatty acyl-CoA thioesters.

The activity of hBFIT2 (0.34 μM) towards 50 μM butyryl-CoA, lauroyl-CoA, myristoyl-CoA and palmitoyl-CoA (C4, C12, C14, C16, respectively) was measured at pH 7.5 and 37 °C. Palmitic acid and myristic acid, activated as CoA thioesters, are the principle substrates for the mitochondrial β-oxidation pathway and thus, these were chosen for activity testing. Butyryl-CoA and lauroyl-CoA were also tested so to evaluate discrimination against shorter chain acyl-CoA thioesters and thus specificity divergence from the paralog CACH.

A reversed-phase HPLC-based assay was employed so that the consumption of the substrate and formation of the CoA product could be simultaneously and directly monitored. The chromatographies of the reaction solutions, quenched at 30 min and 60 min were monitored at 260 nm, the wavelength at which the adenine chromophore absorbs maximally. The HPLC chromatograms are shown in Figure 8 along with the chromatograms measured for the control reactions (lacking hBFIT2) sampled at 2 h. At 30 min the catalyzed hydrolysis palmitoyl-CoA was complete and thus, the calculated turnover rate of this substrate is greater than 5 min^{-1}. At 30 min, 36 μM of the 50 μM myristoyl-CoA had been hydrolyzed therefore setting the turnover rate equal to or slightly greater than 3.5 min^{-1}. Lauroyl-CoA (24 μM consumed at 30 min) and butyryl-CoA (13 μM consumed at 60 min) displayed slower turnover rates of 2.3 min^{-1} and 0.2 min^{-1}, respectively. Based on the relative rates of hydrolysis we conclude that hBFIT2 is targeting long chain fatty acyl-CoA thioesters. This substrate preference contrasts that of the CACH, which has been reported to be most active with acetyl-CoA (48).

The START Domain

The hBFIT2 StarD14 domain (Figure 1C) and the hCACH StarD15 domain share 43% sequence identity. In contrast, these domains share less than 15% sequence identity with the other human START proteins. In the present study, we used a protein-lipid overlay assay to test lipid binding with hBFIT2 (0.5 μg/mL hBFIT2) and hCACH (0.1 μg/mL). As a control we used the hotdog-fold thioesterase ybdB (6 μg/mL) from *E. coli*, which was selected in part because BFIT2 and ybdB belong to the same clade of hotdog-fold thioesterases and in part because ybdB is a promiscuous thioesterase, and included among its *in-vitro* substrates are fatty acyl-CoA thioesters (47). Both hBFIT2 and hCACH displayed specific binding with the phosphatidyl inositol-4-phosphate sample (Figure 9). The stronger signal observed for hBFIT2 is likely due to its 5-fold higher concentration. The ybdB, which was used at a 60-fold higher concentration, revealed little-to-no binding interaction. These results indicate that in the cell, the StarD14 and StarD15 domains might associate with phosphatidyl inositol-4-phosphate or perhaps, just with the inositol-4-phosphate head-group. To test the feasibility of phosphatidyl inositol-4-phosphate binding, we modeled its polar head group into the binding site of the StarD14 domain using the program COOT (54) and found that several polar binding interactions are possible (Figure SI4). However, it would be premature to make any firm conclusions. Future work, which includes *in-vitro* titration with the

phosphatidyl inositol-4-phosphate must be first carried out to measure the binding curve and thereby determine the actual binding constant.

Conclusions

The assignment of the biological functions of the human thioesterases presents a challenge that must be met in order to better understand the regulation of lipid metabolism and its role in lipid-related diseases. The majority of the human thioesterases belong to the hotdog-fold family. Our earlier focus on the structure-function relationships among bacterial hotdog-fold thioesterases has provided us with a platform for tackling the complexities associated with human thioesterase function assignment. Based on our own work, and the work of numerous other investigators, it has become clear that the hotdog-fold thioesterases are limited to CoA or holo-acyl carrier proteins (ACP) thioester substrates because of the topology of the substrate binding site that is set by the conserved fold. Briefly, this fold accommodates the nucleotide or ACP unit on the protein surface at the entrance of a long, narrow tunnel that ultimately leads to the catalytic site. The pantetheine arm threads through the tunnel wherein a combination of desolvation and electrostatic interactions provide a signification fraction of the substrate binding energy. Consequently, some thioesterases are able to hydrolyze both CoA and *holo*ACP thioesters. The pantetheine binding tunnel opens to the catalytic site, which can be enclosed for specific substrate targeting (55) or open to allow substrates with varying sized acyl or aroyl groups to bind (21, 30). In the present study, we showed that hBFIT2 catalyzes the *in-vitro* hydrolysis of fatty acyl-CoA thioesters with a preference for long chains (C14-C16) over shorter chains.

The demonstration of hBFIT2 fatty acyl-CoA thioesterase activity and its localization to the mitochondrial matrix is only the first step in assigning biological function. Notably, hBFIT2 is not the only thioesterase present in the matrix (56-57). The presence of the StarD14 domain in hBFIT suggests that the thioesterase activity is subject to a unique form of regulation, or alternatively that hBFIT performs a biochemical function that extends beyond that of a thioesterase.

Supplementary Material

Refer to Web version on PubMed Central for supplementary material.

References

1. Lowell BB, Spiegelman BM. Towards a molecular understanding of adaptive thermogenesis. Nature. 2000; 404:652–660. [PubMed: 10766252]
2. Butow RA, Bahassi EM. Adaptive thermogenesis: orchestrating mitochondrial biogenesis. Curr Biol. 1999; 9:R767–769. [PubMed: 10531019]
3. Lowell BB. Adaptive thermogenesis: turning on the heat. Curr Biol. 1998; 8:R517–520. [PubMed: 9705924]
4. Puigserver P, Wu Z, Park CW, Graves R, Wright M, Spiegelman BM. A cold-inducible coactivator of nuclear receptors linked to adaptive thermogenesis. Cell. 1998; 92:829–839. [PubMed: 9529258]
5. Nedergaard J, Golozoubova V, Matthias A, Asadi A, Jacobsson A, Cannon B. UCP1: the only protein able to mediate adaptive non-shivering thermogenesis and metabolic inefficiency. Biochim Biophys Acta. 2001; 1504:82–106. [PubMed: 11239487]

6. Ricquier D. Neonatal brown adipose tissue, UCP1 and the novel uncoupling proteins. Biochem Soc Trans. 1998; 26:120–123. [PubMed: 9649731]
7. Nedergaard J, Matthias A, Golozoubova V, Jacobsson A, Cannon B. UCP1: the original uncoupling protein--and perhaps the only one? New perspectives on UCP1, UCP2, and UCP3 in the light of the bioenergetics of the UCP1-ablated mice. J Bioenerg Biomembr. 1999; 31:475–491. [PubMed: 10653476]
8. Matthias A, Ohlson KB, Fredriksson JM, Jacobsson A, Nedergaard J, Cannon B. Thermogenic responses in brown fat cells are fully UCP1-dependent. UCP2 or UCP3 do not substitute for UCP1 in adrenergically or fatty scid-induced thermogenesis. J Biol Chem. 2000; 275:25073–25081. [PubMed: 10825155]
9. Ribeiro MO, Lebrun FL, Christoffolete MA, Branco M, Crescenzi A, Carvalho SD, Negrao N, Bianco AC. Evidence of UCP1-independent regulation of norepinephrine-induced thermogenesis in brown fat. Am J Physiol Endocrinol Metab. 2000; 279:E314–322. [PubMed: 10913031]
10. Yu XX, Lewin DA, Forrest W, Adams SH. Cold elicits the simultaneous induction of fatty acid synthesis and beta-oxidation in murine brown adipose tissue: prediction from differential gene expression and confirmation in vivo. FASEB J. 2002; 16:155–168. [PubMed: 11818363]
11. Watanabe M, Yamamoto T, Mori C, Okada N, Yamazaki N, Kajimoto K, Kataoka M, Shinohara Y. Cold-induced changes in gene expression in brown adipose tissue: implications for the activation of thermogenesis. Biol Pharm Bull. 2008; 31:775–784. [PubMed: 18451493]
12. Zhang Y, Li Y, Niepel MW, Kawano Y, Han S, Liu S, Marsili A, Larsen PR, Lee CH, Cohen DE. Targeted deletion of thioesterase superfamily member 1 promotes energy expenditure and protects against obesity and insulin resistance. Proc Natl Acad Sci U S A. 2012; 109:5417–5422. [PubMed: 22427358]
13. Nedergaard J, Bengtsson T, Cannon B. Unexpected evidence for active brown adipose tissue in adult humans. Am J Physiol Endocrinol Metab. 2007; 293:E444–452. [PubMed: 17473055]
14. Bartelt A, Heeren J. The holy grail of metabolic disease: brown adipose tissue. Curr Opin Lipidol. 2012; 23:190–195. [PubMed: 22449813]
15. Hu HH, Tovar JP, Pavlova Z, Smith ML, Gilsanz V. Unequivocal identification of brown adipose tissue in a human infant. J Magn Reson Imaging. 2012; 35:938–942. [PubMed: 22180228]
16. Ponting CP, Aravind L. START: a lipid-binding domain in StAR, HD-ZIP and signalling proteins. Trends Biochem Sci. 1999; 24:130–132. [PubMed: 10322415]
17. Alpy F, Tomasetto C. Give lipids a START: the StAR-related lipid transfer (START) domain in mammals. J Cell Sci. 2005; 118:2791–2801. [PubMed: 15976441]
18. Li Z, Song F, Zhuang Z, Dunaway-Mariano D, Anderson KS. Monitoring enzyme catalysis in the multimeric state: direct observation of Arthrobacter 4-hydroxybenzoyl-coenzyme A thioesterase catalytic complexes using time-resolved electrospray ionization mass spectrometry. Anal Biochem. 2009; 394:209–216. [PubMed: 19635449]
19. Zhao H, Martin BM, Bisoffi M, Dunaway-Mariano D. The Akt C-terminal modulator protein is an acyl-CoA thioesterase of the Hotdog-Fold family. Biochemistry. 2009; 48:5507–5509. [PubMed: 19453107]
20. Cao J, Xu H, Zhao H, Gong W, Dunaway-Mariano D. The mechanisms of human hotdog-fold thioesterase 2 (hTHEM2) substrate recognition and catalysis illuminated by a structure and function based analysis. Biochemistry. 2009; 48:1293–1304. [PubMed: 19170545]
21. Zhuang Z, Song F, Zhao H, Li L, Cao J, Eisenstein E, Herzberg O, Dunaway-Mariano D. Divergence of function in the hot dog fold enzyme superfamily: the bacterial thioesterase YciA. Biochemistry. 2008; 47:2789–2796. [PubMed: 18247525]
22. Song F, Zhuang Z, Finci L, Dunaway-Mariano D, Kniewel R, Buglino JA, Solorzano V, Wu J, Lima CD. Structure, function, and mechanism of the phenylacetate pathway hot dog-fold thioesterase PaaI. J Biol Chem. 2006; 281:11028–11038. [PubMed: 16464851]
23. Zhuang Z, Song F, Takami H, Dunaway-Mariano D. The BH1999 protein of Bacillus halodurans C-125 is gentisyl-coenzyme A thioesterase. J Bacteriol. 2004; 186:393–399. [PubMed: 14702308]
24. Thoden JB, Zhuang Z, Dunaway-Mariano D, Holden HM. The structure of 4-hydroxybenzoyl-CoA thioesterase from arthrobacter sp. strain SU. J Biol Chem. 2003; 278:43709–43716. [PubMed: 12907670]

25. Zhuang Z, Gartemann KH, Eichenlaub R, Dunaway-Mariano D. Characterization of the 4-hydroxybenzoyl-coenzyme A thioesterase from Arthrobacter sp. strain SU. Appl Environ Microbiol. 2003; 69:2707–2711. [PubMed: 12732540]
26. Zhuang Z, Song F, Zhang W, Taylor K, Archambault A, Dunaway-Mariano D, Dong J, Carey PR. Kinetic, Raman, NMR, and site-directed mutagenesis studies of the Pseudomonas sp. strain CBS3 4-hydroxybenzoyl-CoA thioesterase active site. Biochemistry. 2002; 41:11152–11160. [PubMed: 12220180]
27. Thoden JB, Holden HM, Zhuang Z, Dunaway-Mariano D. X-ray crystallographic analyses of inhibitor and substrate complexes of wild-type and mutant 4-hydroxybenzoyl-CoA thioesterase. J Biol Chem. 2002; 277:27468–27476. [PubMed: 11997398]
28. Benning MM, Wesenberg G, Liu R, Taylor KL, Dunaway-Mariano D, Holden HM. The three-dimensional structure of 4-hydroxybenzoyl-CoA thioesterase from Pseudomonas sp. Strain CBS-3. J Biol Chem. 1998; 273:33572–33579. [PubMed: 9837940]
29. Zhuang Z, Latham J, Song F, Zhang W, Trujillo M, Dunaway-Mariano D. Investigation of the catalytic mechanism of the hotdog-fold enzyme superfamily Pseudomonas sp. strain CBS3 4-hydroxybenzoyl-CoA thioesterase. Biochemistry. 2012; 51:786–794. [PubMed: 22208697]
30. Willis MA, Zhuang Z, Song F, Howard A, Dunaway-Mariano D, Herzberg O. Structure of YciA from Haemophilus influenzae (HI0827), a hexameric broad specificity acyl-coenzyme A thioesterase. Biochemistry. 2008; 47:2797–2805. [PubMed: 18260643]
31. Kirkby B, Roman N, Kobe B, Kellie S, Forwood JK. Functional and structural properties of mammalian acyl-coenzyme A thioesterases. Prog Lipid Res. 2010; 49:366–377. [PubMed: 20470824]
32. Adams SH, Chui C, Schilbach SL, Yu XX, Goddard AD, Grimaldi JC, Lee J, Dowd P, Colman S, Lewin DA. BFIT, a unique acyl-CoA thioesterase induced in thermogenic brown adipose tissue: cloning, organization of the human gene and assessment of a potential link to obesity. Biochem J. 2001; 360:135–142. [PubMed: 11696000]
33. Li J, Derewenda U, Dauter Z, Smith S, Derewenda ZS. Crystal structure of the Escherichia coli thioesterase II, a homolog of the human Nef binding enzyme. Nat Struct Biol. 2000; 7:555–559. [PubMed: 10876240]
34. Keatinge-Clay A. Crystal structure of the erythromycin polyketide synthase dehydratase. J Mol Biol. 2008; 384:941–953. [PubMed: 18952099]
35. Kotaka M, Kong R, Qureshi I, Ho QS, Sun H, Liew CW, Goh LP, Cheung P, Mu Y, Lescar J, Liang ZX. Structure and catalytic mechanism of the thioesterase CalE7 in enediyne biosynthesis. J Biol Chem. 2009; 284:15739–15749. [PubMed: 19357082]
36. Koski MK, Haapalainen AM, Hiltunen JK, Glumoff T. A two-domain structure of one subunit explains unique features of eukaryotic hydratase 2. J Biol Chem. 2004; 279:24666–24672. [PubMed: 15051722]
37. Kato JY, Funa N, Watanabe H, Ohnishi Y, Horinouchi S. Biosynthesis of gamma-butyrolactone autoregulators that switch on secondary metabolism and morphological development in Streptomyces. Proc Natl Acad Sci U S A. 2007; 104:2378–2383. [PubMed: 17277085]
38. Akula N, Midzak A, Lecanu L, Papadopoulos V. Identification of small-molecule inhibitors of the steroidogenic acute regulatory protein (STARD1) by structure-based design. Bioorg Med Chem Lett. 2012; 22:4139–4143. [PubMed: 22575868]
39. Borthwick F, Taylor JM, Bartholomew C, Graham A. Differential regulation of the STARD1 subfamily of START lipid trafficking proteins in human macrophages. FEBS Lett. 2009; 583:1147–1153. [PubMed: 19272380]
40. Roderick SL, Chan WW, Agate DS, Olsen LR, Vetting MW, Rajashankar KR, Cohen DE. Structure of human phosphatidylcholine transfer protein in complex with its ligand. Nat Struct Biol. 2002; 9:507–511. [PubMed: 12055623]
41. Rigotti A, Cohen DE, Zanlungo S. STARTing to understand MLN64 function in cholesterol transport. J Lipid Res. 2010; 51:2015–2017. [PubMed: 20511492]
42. Watari H, Arakane F, Moog-Lutz C, Kallen CB, Tomasetto C, Gerton GL, Rio MC, Baker ME, Strauss JF 3rd. MLN64 contains a domain with homology to the steroidogenic acute regulatory

protein (StAR) that stimulates steroidogenesis. Proc Natl Acad Sci U S A. 1997; 94:8462–8467. [PubMed: 9237999]

43. Horibata Y, Sugimoto H. StarD7 mediates the intracellular trafficking of phosphatidylcholine to mitochondria. J Biol Chem. 2010; 285:7358–7365. [PubMed: 20042613]
44. Angeletti S, Maggio B, Genti-Raimondi S. Surface activity and interaction of StarD7 with phospholipid monolayers. Biochem Biophys Res Commun. 2004; 314:181–185. [PubMed: 14715263]
45. Kudo N, Kumagai K, Tomishige N, Yamaji T, Wakatsuki S, Nishijima M, Hanada K, Kato R. Structural basis for specific lipid recognition by CERT responsible for nonvesicular trafficking of ceramide. Proc Natl Acad Sci U S A. 2008; 105:488–493. [PubMed: 18184806]
46. Thorsell AG, Lee WH, Persson C, Siponen MI, Nilsson M, Busam RD, Kotenyova T, Schuler H, Lehtio L. Comparative structural analysis of lipid binding START domains. PLoS One. 2011; 6:e19521. [PubMed: 21738568]
47. Chen D, Wu R, Bryan TL, Dunaway-Mariano D. In vitro kinetic analysis of substrate specificity in enterobactin biosynthetic lower pathway enzymes provides insight into the biochemical function of the hot dog-fold thioesterase EntH. Biochemistry. 2009; 48:511–513. [PubMed: 19119850]
48. Suematsu N, Isohashi F. Molecular cloning and functional expression of huma cytosolic acetyl-CoA hydrolase. Acta Biochim Pol. 2006; 53:553–561. [PubMed: 16951743]
49. von Heijne G. Mitochondrial targeting sequences may form amphiphilic helices. EMBO J. 1986; 5:1335–1342. [PubMed: 3015599]
50. Omura T. Mitochondria-targeting sequence, a multi-role sorting sequence recognized at all steps of protein import into mitochondria. J Biochem. 1998; 123:1010–1016. [PubMed: 9603986]
51. Herrmann JM, Hell K. Chopped, trapped or tacked--protein translocation into the IMS of mitochondria. Trends Biochem Sci. 2005; 30:205–211. [PubMed: 15817397]
52. Klaus S, Keipert S, Rossmeisl M, Kopecky J. Augmenting energy expenditure by mitochondrial uncoupling: a role of AMP-activated protein kinase. Genes Nutr. 2012; 7:369–386. [PubMed: 22139637]
53. Suematsu N, Okamoto K, Isohashi F. Mouse cytosolic acetyl-CoA hydrolase, a novel candidate for a key enzyme involved in fat metabolism: cDNA cloning, sequencing and functional expression. Acta Biochim Pol. 2002; 49:937–945. [PubMed: 12545200]
54. Emsley P, Cowtan K. Coot: model-building tools for molecular graphics. Acta Crystallogr D Biol Crystallogr. 2004; 60:2126–2132. [PubMed: 15572765]
55. Weeks AM, Coyle SM, Jinek M, Doudna JA, Chang MC. Structural and biochemical studies of a fluoroacetyl-CoA-specific thioesterase reveal a molecular basis for fluorine selectivity. Biochemistry. 2010; 49:9269–9279. [PubMed: 20836570]
56. Brocker C, Carpenter C, Nebert DW, Vasiliou V. Evolutionary divergence and functions of the human acyl-CoA thioesterase gene (ACOT) family. Hum Genomics. 2010; 4:411–420. [PubMed: 20846931]
57. Kirkby B, Roman N, Kobe B, Kellie S, Forwood JK. Functional and structural properties of mammalian acyl-coenzyme A thioesterases. Prog Lipid Res. 2010; 49:366–77. [PubMed: 20470824]

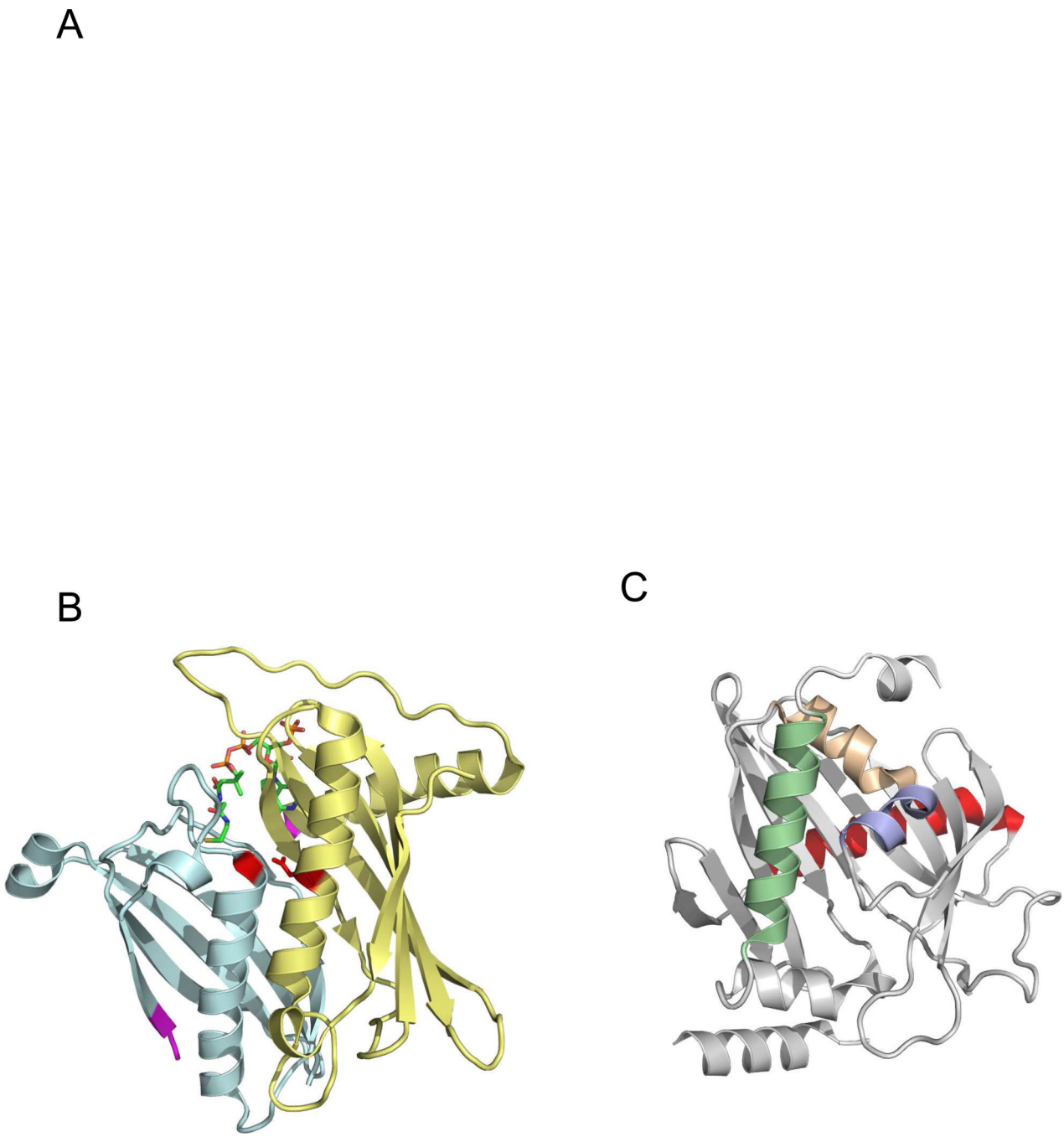

Figure 1.

(A) A diagram of the domain organization in human BFIT2 and the two human BFIT2 gene constructs that were used in this work. N-term corresponds to the MLS, HD-THIO to the hotdog-fold domain, START to the StarD14 domain. (**B**) One subunit of the trimeric human CACH (ACOT12) double hotdog-fold unit (PDB ID: 3B7K). The first hotdog-fold domain is colored pale yellow and the second hotdog domain is colored pale cyan. The residues 151-180, which form the domain-domain linker, are disordered and are therefore not shown in the structure. Residues 150 and 181 are colored magenta. A CoA ligand, bound to one of

the two active sites, is shown in stick with carbon atoms colored green, nitrogen atoms blue, oxygen atoms red and the sulfur atom yellow. The posited catalytic residues Gly202 and Asp36 are colored red. (**C)** The BFIT2 START domain StarD14 (PDB ID: 3FO5). The conserved α-helices are colored. The gate-keeper α-helix 4 is colored pale green.

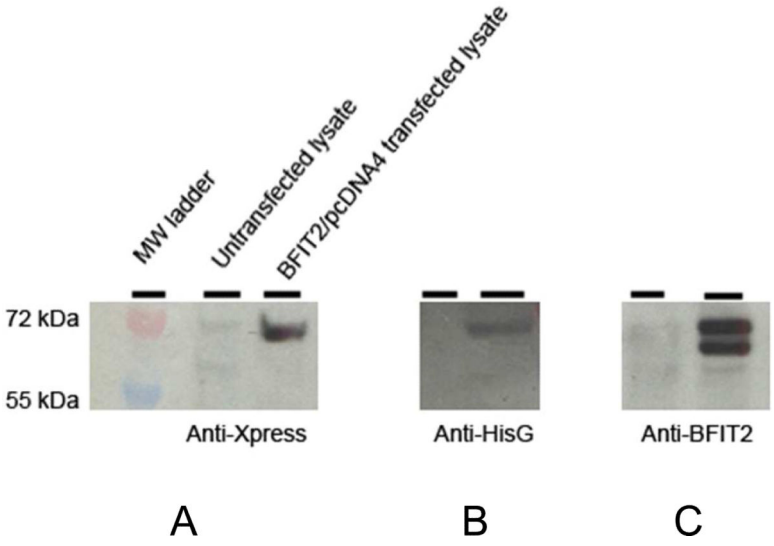

Figure 2.

Immunoblot of untransfected (middle or left lane) and *hBFIT2/pcDNA4 transfected* HEK293T/17 cell lysates (right lane) using anti-Xpress antibody (**A**), anti-HisG antibody (**B**) and anti-BFIT2 antibody (**C**).

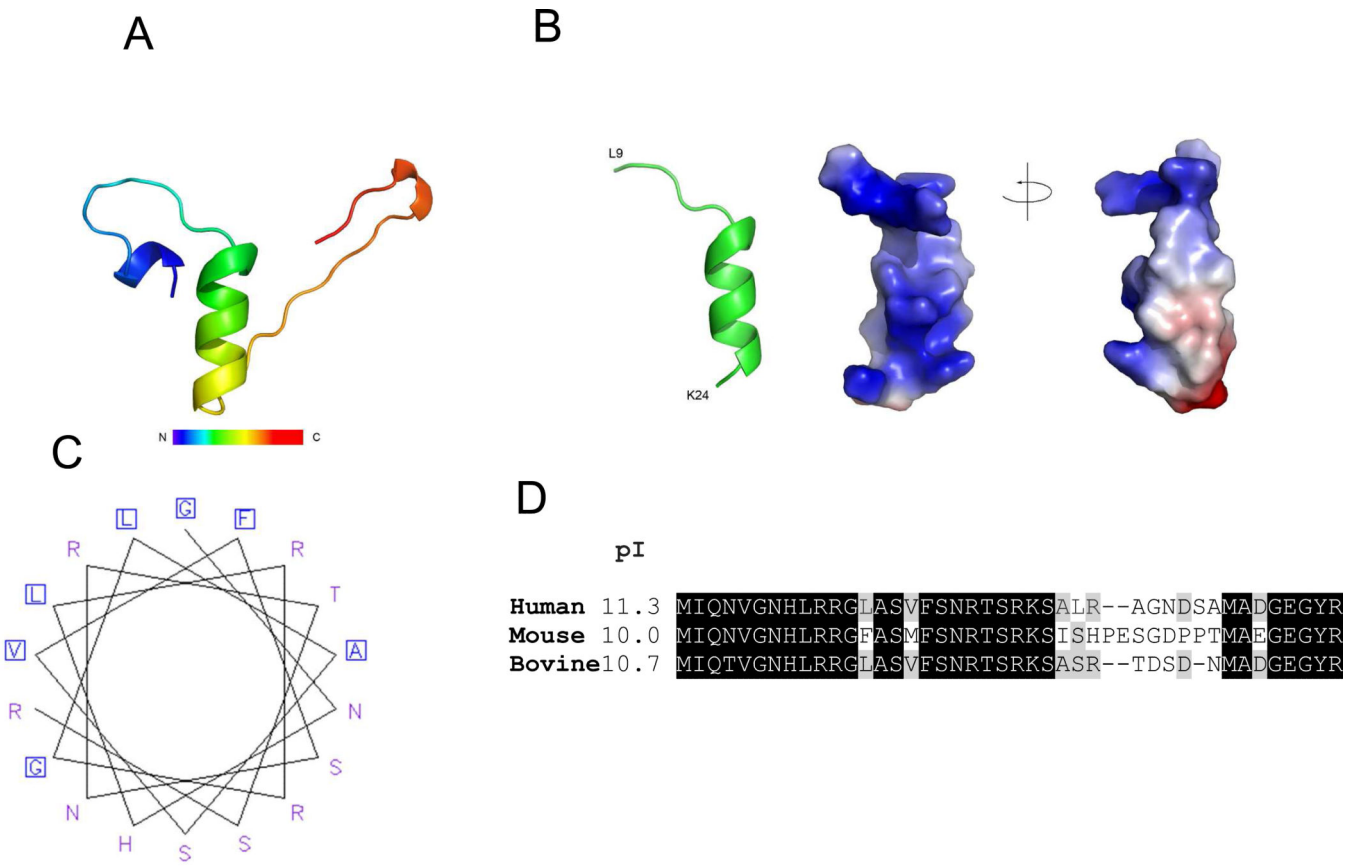

Figure 3.

(**A**) Predicted tertiary structure of the hBFIT2 N-terminal region (residues 1-42). (**B**) Electrostatic vacuum surface of the central α-helix (hBFIT2 residues 9-24). (**C**) EMBOSS pepwheel diagram of hBFIT2 residues 5-24. (**D**) Sequence alignment and estimated pI value of the N-terminal region of BFIT2 from various mammalian species.

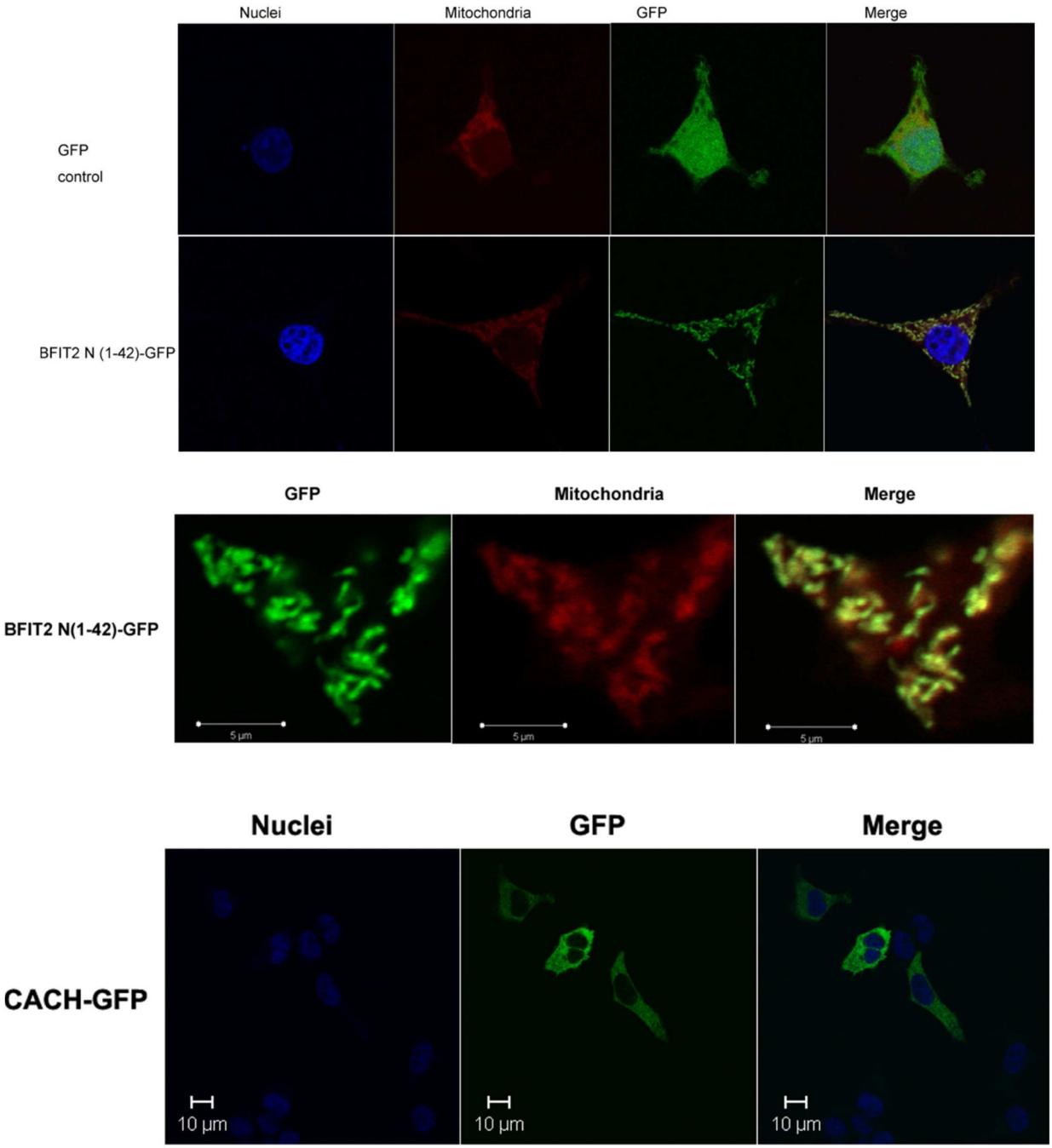

Figure 4.

(Top) Confocal imaging of the GFP and BFIT2 N(1-42)-GFP in transfected HEK 293T/17 cells. (Center) Zoom-in on the fluorescence from the BFIT2 N(1-42)-GFP and the mitochondria dyed with mitotracker CMXRos. (Bottom) Confocal imaging of CACH-GFP showing distributive localization in the transfected HEK 293T/17 cells. The nuclei were stained by Hoechst 33342.

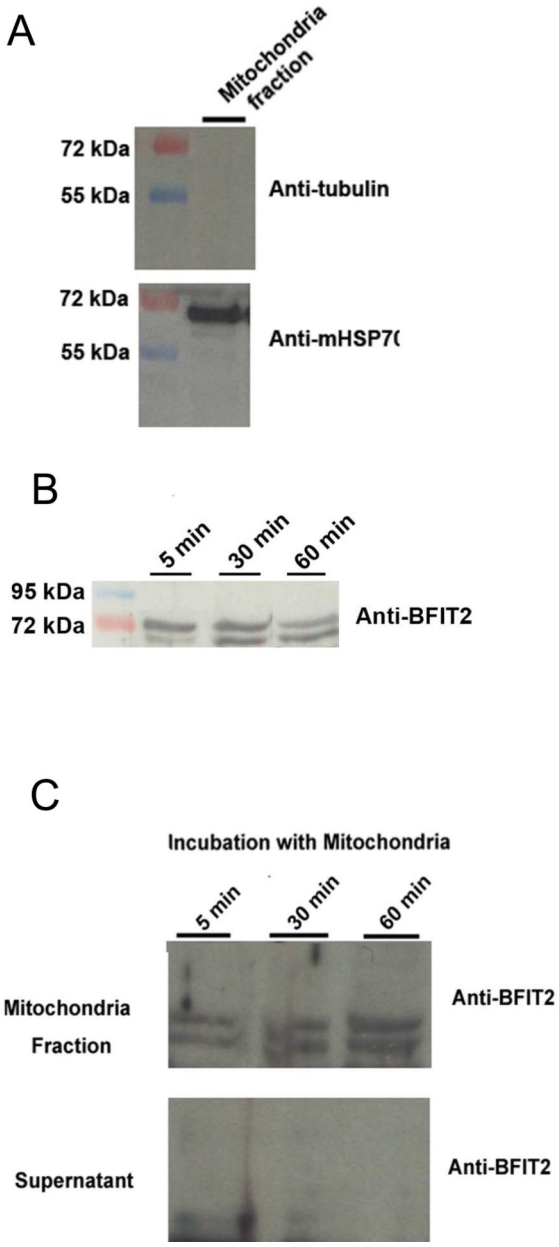

Figure 5.

In-vitro mitochondrial processing and importing of precursor hBFIT2. **A**. Immunoblot of the mitochondrial fraction of HEK/293 cells using the anti-mHSP70 antibody and the anti-α-tubulin antibody. The mHSP70 (71 kDa) is the mitochondrial marker and α-tubulin (50 kDa) is the cytosolic marker. The mitochondrial fraction is free of cytosol contamination. **B**. Immunoblot of precursor hBFIT2 treated with the mitochondria in mannitol buffer for 5, 30 and 60 min. The anti-hBFIT2 antibody was used to detect the precursor (upper band) and mature (lower band) forms of hBFIT2. **C**. Immunoblot of the mitochondrial and supernatant fractions derived from centrifugation of the reaction mixtures from (B). The anti-hBFIT2 antibody was used to detect the precursor (upper band) and mature (lower band) forms of

hBFIT2. The precursor hBFIT2 was taken up by the mitochondria and processed to the mature form.

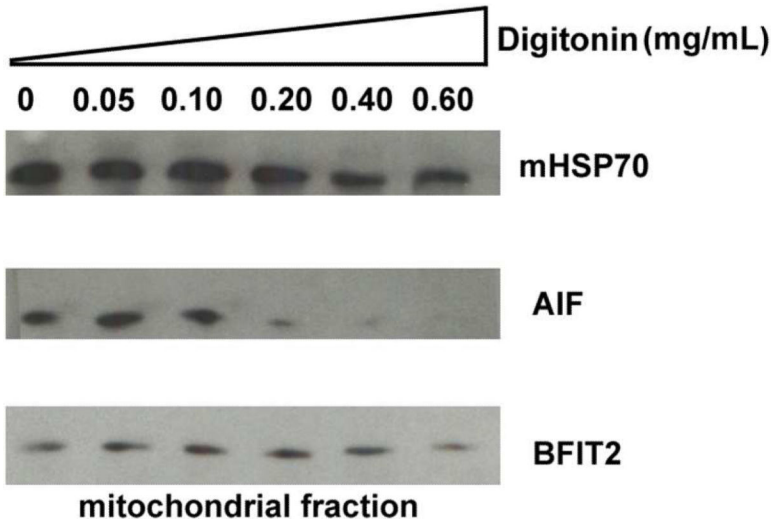

Figure 6.

Immunoblot analysis of the digitonin-induced release of the mitochondrial intermembrane compartment marker protein AlF (with anti-ALF antibody), the mitochondrial matrix marker protein mHSP70 (with anti-mHSP70 antibody) and hBFIT2 (with anti-Xpress antibody) from mitochondria isolated from *hBFIT2/pcDNA4* transfected HEK293T/17 cells.

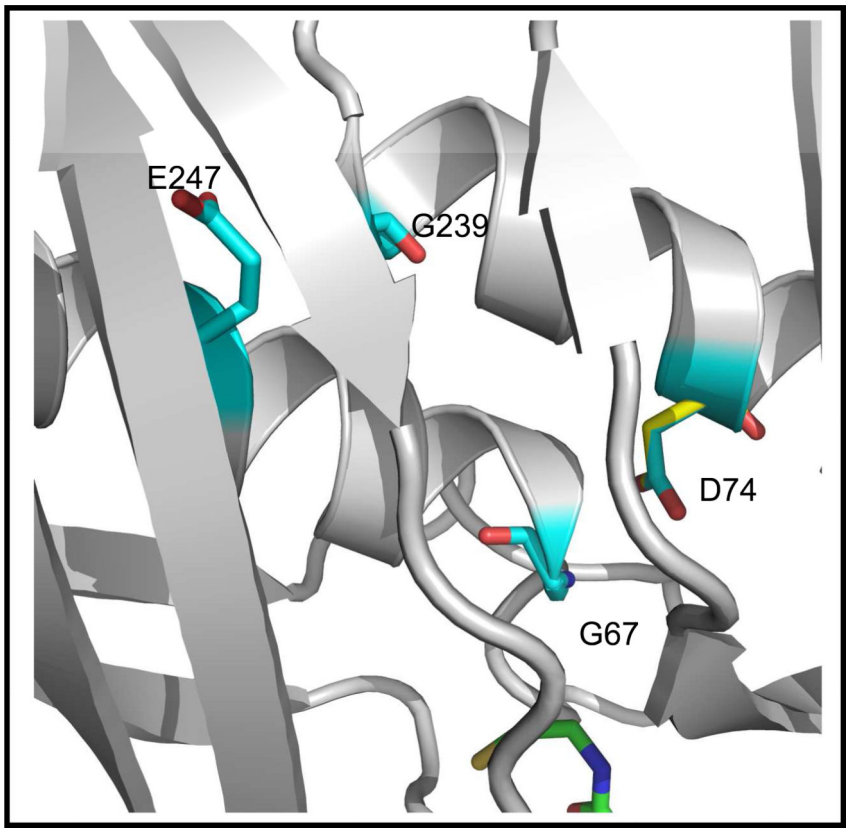

Figure 7.

A snapshot of the two active sites of the double hotdog-fold unit of hBFIT2 modeled in PHYRE2 using the double hotdog-fold unit of CACH (ACOT12) (PDB ID: 3B7K), which shares 60% sequence identity, as the template. The thiol end of the superimposed CACH CoA ligand is shown at the bottom of the figure in stick using the same coloring pattern used in Figure 1B. The putative hBFIT2 catalytic residues are shown in stick with carbon atoms colored cyan, oxygen atoms red and nitrogen atoms in blue. The corresponding residues of the superimposed CACH (carbon atoms colored yellow) are coincident.

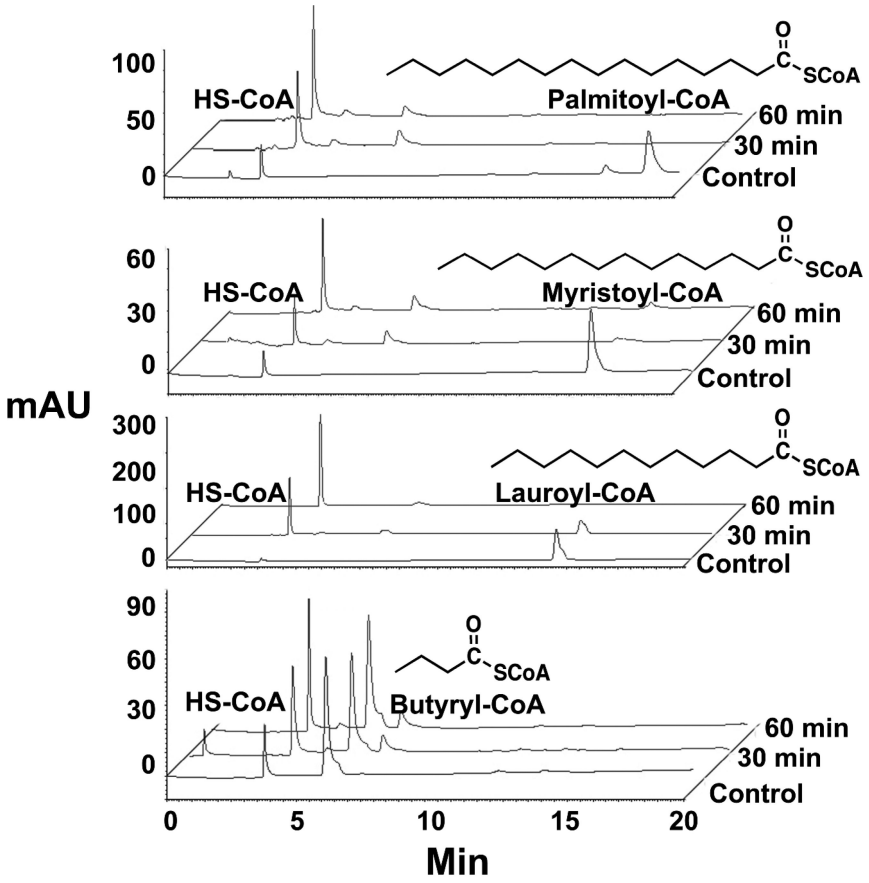

Figure 8.

Reversed-phase HPLC chromatograms of reactions mixtures initially containing 0.34 μM purified recombinant hBFIT2 and 50 μM fatty acyl-CoA substrate in 50 mM HEPES buffer (pH 7.5, 37 °C). Aliquots were removed at 30 min and 60 min incubation periods for analysis. The control reactions, which lacked hBFIT2, were incubated for 2 h. See Materials and Methods for details.

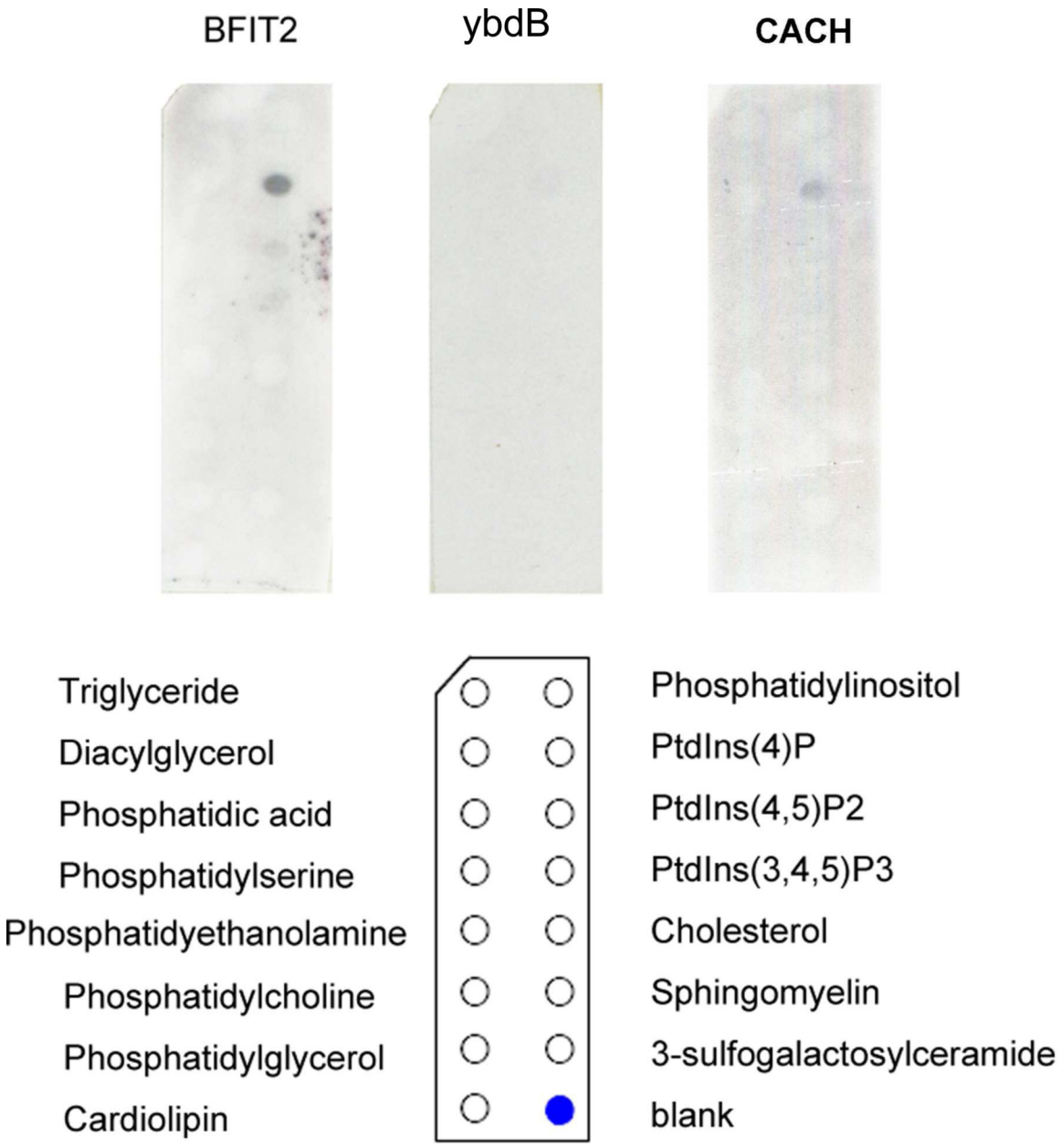

Figure 9.

Protein-lipid overlay assays in which Membrane Lipid Strips (Echelon Bioscience Inc.) were separately treated 0.5 μg/mL hBFIT2 (purified as described above), 0.1 μg/mL hCACH or 6 μg/mL HisG and Xpress-tagged ybdB in PBS-T and then imaged. See Materials and Methods. The lipid positions are identified in the key provided.